CONTROLLED RELEASE OF FERTILISER USING MESOPOROUS SILICA NANOPARTICLES

H. Wanyika[1], E. Gatebe[2], P. Kioni[3], Z. Tang[4] and Y. Gao[5]
[1,2]Department of Chemistry, Jomo Kenyatta University of Agriculture and Technology, Nairobi, Kenya
[3]Kimathi University College of Technology, Nyeri, Kenya
[4,5]National Centre for Nano-science and Technology, Beijing, China
E-mail: eujed@yahoo.com

Abstract
Nanostructured delivery systems for fertilizers could minimize leaching and consequently reduce the amounts applied. In this study, Mesoporous Silica Nanoparticles (MSNs) were explored as controlled release carriers for fertilizers. A series of MSNs with particle sizes, Barrett-Joyner-Halenda (BJH) pore diameters, Brunauer-Emmett-Teller (BET) surface areas and BJH total pore volumes ranging between 50 nm – 900 nm, 2.4 nm - 4.4 nm, 589 m^2g^{-1} - 1013 m^2g^{-1} and 0.61 cm^3g^{-1} – 0.81 cm^3g^{-1} respectively were synthesized via Liquid Crystal Templating Mechanism (LCT). Urea was used as a model fertilizer to access the fertilizer loading and controlled release behaviour of MSNs. Loading was achieved by a simple immersion technique using concentrated aqueous urea solution. As much as 19.8 % - 78.2 % of the MSNs surface areas and 16.8 % - 99.0 % of the mesopore volumes were loaded with urea molecules, mainly by physisorption. *In vitro* release studies of urea-loaded MSNs (UMSNs) in water indicated a burst release (32 % - 91 %) within the 1st day attributed to the urea adsorbed on the external surfaces, followed by a slow and sustained release for up to 6 days when all urea was released (100 %), ascribed to urea molecules entrapped in the mesopores. The release profiles were found to vary with the physical properties of MSNs. Great potential for the development of fertilizer nanocarrier systems based on MSNs was revealed.

Key words: Mesoporous silica nanoparticles (MSNs), controlled release (CR), urea-loaded MSNs (UMSNs)

1.0 Introduction

Considerable loss through leaching, surface migration and decomposition of the agrochemicals triggered by such factors like sunlight, rain and wind have greatly compromised the efficacy of fertilizers, and therefore periodic application is required for satisfactory treatment.

Nanotechnology which is the manipulation of materials at atomic and molecular level is a generic technology that offers better-built, safer, long-lasting, cheap and smart products. It could have important impact in novel agricultural and food security systems and environmental protection (Miller *et al*., 2005).

MSNs have been intensively explored in nanotechnology research due to their unique properties, such as high surface areas, large pore volumes, tunable pore sizes with a narrow distribution and tunable particle diameters (Bottini *et al*., 2007, Gerion *et al*., 2007, Graf *et al*., 2006). Zhu and co-workers demonstrated the biocompatibility, the high structural stability and chemical versatility of silica (Zhu *et al*., 2007). Furthermore, the biodegradability and non-toxicity of silica particles has been shown (Popat *et al*., 2011). In this regard, MSNs are undoubtfully excellent candidates for drug delivery systems. Beck *et al.* (1992) described the liquid crystal templating (LCT) mechanism for the synthesis of MSNs. Various types of surfactants are used as structure-directing agents in this novel synthesis (Gao *et al*., 2006). The inter molecular bonding interactions play a major role in the templating mechanism which takes place under a wide range of pH and temperature conditions (Liu *et al*., 2011).

Recently, nanotechnology research has given great focus to development of drug nanocarriers with controlled release (CR) properties. Various researchers have attempted to study agrochemical controlled release systems based on silica. Wen *et al*., (2005) employed porous hollow silica nanoparticles (PHSNs) as pesticide carriers to study the controlled release behaviour of avermectin pesticide. They observed that the PHSNs carriers markedly delayed the release of the pesticide and concluded that that PHSN can be exploited in controlled pesticide delivery application. Other researchers reported a slow-release formulation of a new biological pesticide pyoluteorin with mesoporous silica. Their novel formulation could release the pesticide in a slow and steady manner (Chen *et al*., 2011). Toxicity bioassays by Madliger *et al*., (2011) demonstrated that transgenic insecticidal Cry1Ab protein adsorbed on silica particles, a major soil constituent retained its insecticidal activity. While a little attempt have been made to study pesticides controlled delivery systems based on MSNs, rare work about fertilizer delivery systems based on nanoparticles has been done. However, slow release formulations for fertilizers based on polymers have been reported (Kale *et al*., 2011). CR formulations of fertilizers can meet the need for prolonged and better control of the agricultural drugs by among others allowing the reduction of the applied amounts (Cotterill and Wilkins, 1996). More Smart nanocarriers can facilitate targeted delivery.

In the current study, MSNs with varied physical properties, that is, particle sizes, pore diameters, pore volumes and surface areas were synthesized by the LCT mechanism using cetyltrimethylammonium bromide (CTAB) as a template surfactant and tetraethyl orthosilicate (TEOS) as a silica precursor in basic conditions. Loading of urea molecules into the MSNs was achieved following a simple and fast procedure of dipping and suspending the nanomaterials in aqueous urea solution. Slow release was triggered by soaking the loaded nanomaterials in distilled water for specified duration of time. The materials acted as potential delivery systems since they exhibited high loading capacities of the guest molecule and slow release.

2.0 Materials and Methods

All the chemicals used in this study were of high purity, at least analytical grade reagents. CTAB, TEOS (SiO_2>28.0%), and Sodium hydroxide (>96%) were purchased from Sigma-Aldrich, UK. All the reagents were used as purchased without further purification. Water used in the experiments was purified by Millipore Milli-Q system to a resistivity of 18.2mΩ.

2.1 Synthesis of Mesoporous Silica Nanoparticles

MSNs were synthesised with modifications to literature procedures (Beck *et al*., 1992; Liu *et al*., 2011). Various samples were prepared from reaction mixtures with different molar compositions of reagents as outlined in Table 1. CTAB was dissolved in nanopure water. Aqueous NaOH was added to the CTAB solution, and the solution temperature was adjusted to 80 ^{O}C in a silicon oil bath with stirring using a magnetic stirrer at 800 rotations per

minute. The solution was heated for 30 minutes after which TEOS was added drop wise, and the mixture was allowed to stir for 2 hours at 80 ^{0}C. The resultant white precipitate was isolated by vacuum filtration using a Buckner funnel and washed several times with copious amount of water. The product was dried in an oven for 2 hours at 140^{O}C and ground into powder using a pestle and a mortar. Calcination of the material was performed at 550 ^{0}C for 5 hours to remove the template.

Table 1 : Molar sol compositions for MSNs syntheses

	Molar sol composition			
Sample code	CTAB (mM)*	TEOS (mM)	NaOH (mM)	H_2O (moles)
MSN - 1 (a)	2.74	27.09	7.0	21.11
MSN - 2 (b)	2.74	27.09	7.0	26.67
MSN - 3 (c)	2.74	27.09	14.0	26.67
MSN - 4 (d)	2.74	27.09	3.8	21.11
MSN - 5 (e)	2.74	27.09	7.6	42.22

*mM – millimoles

2.2 Loading of Mesoporous Silica Nanoparticles with Urea

Urea was chosen as a model fertilizer to assess the drug loading and controlled release behaviour of MSNs. To load, concentrated aqueous solution of urea containing 1:2 w/v urea: water was prepared, followed by suspension of ~250mg of MSNs. The urea-MSN (w/w) ratio was selected to be 20:1. The suspensions were stirred at room temperature for 2hours at 300 rotations per minute (rpm) to reach equilibrium. The suspensions were filtered under vacuum, particles washed with copius amount of water and dried in an oven at 60^{O}C for 3 hours. The loaded samples were denoted UMSNs corresponding to respective MSNs.

2.3 Characterisation

SEM images were collected on a scanning electron microscope model Hitachi S4800. TEM images were obtained on a Tecnai G^2 20 S-TWIN transmission electron microscope. Sample preparation was done by dispersing a little amount of sample in pure water. A thin film of the homogenous sample solution was deposited and air dried on the reflective surfaces of silicon wafer for SEM analysis. The sample was casted on carbon coated copper grid for TEM analysis.

Nitrogen adsorption / desorption Isotherms of calcined MSNs and UMSNs powders were collected on an ASAP 2020 Micromeritics equipment at -196^{O}C. The specific surface areas were assessed according to the standard BET method (Brunauer *et al*., 1938). The pore size distributions were calculated from adsorption branches of Isotherms by the BJH method (Barrett *et al*., 1951). FT-IR spectra were obtained using Perkin Elmer Spectrometer (SPECTMM ONE B) in the range 400-4000cm^{-1}. The sample-KBr discs were employed. Powder Small-angle XRD (SAXRD) patterns were recorded on an X'PertPro PANalytical, LR 39487C XRD diffractometer using Cu Kα radiation (40 kV, 40 mA). Stepwise increase was 0.01^O over the range of 1 ^{O} - 8^O 2θ. Samples were prepared as thin layers on glass slides. TGA and DTA were done on a Perkin-Elmer thermal gravimetric analyzer (TGA-7) from RT to 800^{O}C at the heating rate of 5^{O}C min^{-1} in air.

2.4 *In vitro* Release Profile of Urea-loaded Mesoporous Silica Nanoparticles

The static release profiles were studied for a period of 10 days with samples collected and analyzed daily. All the 10 measurements for each sample were started simultaneously. UMSNs (10.0 mg) were accurately weighed. They were suspended in 3 mL of pure water in conical bottles. The suspensions were stirred at 100 rpm at room temperature and centrifuged after every time lapse. Urea released in water was assayed using UV/Vis Spectrophotometry.

2.4.1 Determination of Urea Content

To quantify released urea, 1.0 mL centrate was diluted with 4.0 mL of 10% trichloroacetic acid and reacted with 1.0 mL modified Ehrlich's reagent (modified by dissolving 5.0g p-dimethylaminobenzaldehyde in 20 mL of concentrated HCl, then adding 80 mL of water). UV/Vis absorbance of the samples was measured using a UV/Vis spectrophotometer (model Hitachi U-3010) at 425 nm. The concentration of urea in the solution was determined using the regression equation for the line of best fit of urea calibration standards. The standards (5, 10, 20, 40, 60, 80 and 100 mg/ 100 mL were prepared by serial dilution of the urea stock solution (1000 mg/ 100 mL). The derivatisation procedure for the standards and subsequent absorbance measurement was as described for samples. Blank solution was composed of 1.0 mL of pure water, 4.0 mL of 10% trichloroacetic acid and 1.0 mL of the modified reagent. All the experiments were done in triplicates and the mean of results taken as the result value.

3.0 Results and Discussion

3.1 Microscopy Observations

The images in Figure 1 depict respective SEM and TEM micrographs of MSNs and UMSNs. Electron microscopy studies showed that MSN materials with varied particle sizes and morphologies were formed. It was possible to obtain monodisperse nanoparticles with hexagonal array of mesopores. The honeycomb like structure of MSN was confirmed. This was in good accordance with the expectations based on the work of previous researchers (Kobler *et al*., 2008; Naik *et al*., 2007; Stober *et al*., 1968). The mechanism of MSNs formation was by LCT where CTAB surfactant micelles were believed to have assembled in a hexagonal array of micellar rods forming a template. The TEOS silica precursor underwent hydrolysis upon contact with water to yield the silicate seeds which entered the aqueous region of the template and were stabilized electrostatically, they then condensed to form inorganic silica walls (Hoffman *et al*., 2006; Kobler and Bein, 2008, Beck *et al*., 1992). Finally mesopores were generated on removal of the template by calcination at high temperatures. Cauda and co-workers described the subsequent removal of template as a key step for obtaining accessible mesopores, large surface areas and pore volumes. They argued that, during calcination, condensation of silanol groups (Si-OH) into siloxane (Si-O-Si) bridges took place, thus consolidating the mesoporous structure (Cauda *et al*., 2011). Spherical NPs with narrow particle size distribution of ~150nm in average diameter were obtained from MSN-1 synthesis sol (Figure 1a). However, when the NaOH (aq) concentration in the sol was reduced to 3.8 mM (MSN-4), nanoparticles with uniform size distribution of ~50 nm were obtained (Figure 1d). Increase of the molar concentration of NaOH to 7.6mM coupled with double increase of water to 42.22 moles (MSN-5), resulted in the formation of ~100nm nanospheres (Figure 1e). Use of higher molar concentration of water (MSN-2), led to ~200nm sized particles (Figure 1b). SEM micrograph in Figure 1c corresponds to a scenario where the molar concentration of NaOH (aq) was increased two fold to 14.0mM and H_2O increased to 26.67moles (MSN-3), the results show aggregated particles of ~900nm. The corresponding TEM images show regular hexagonal arrays of uniform channels that are uniformly distributed (Figure 1: f - j).

The relatively low molar concentration of $NaOH_{(aq)}$ used to achieve small monodispersed particles in MSN-4 suggests that the concentration of the morphology catalyst and structure stabilizer has to be kept in a certain ratio with respect to other reagents for high-quality nanoparticles, that is, those with a defined diameter, monodisperse size distribution, and small degree or no agglomeration to be realized. Various methods have been reported in literature to be effective in the control of particle size and agglomeration behavior of nanoparticles in liquid-phase syntheses (Feldmann and Goesmann, 2010). High dilution as it was in MSN-5 has been reported to control nucleus growth and agglomeration by complete separation of the reaction spaces (Feldmann and Goesmann, 2010). Furthermore, high water concentration is absolutely important for complete hydrolysis of TEOS ($Si(OR)_4$, R = C_2H_5), this ensures that all of the OR groups are replaced by OH group, that is, $Si(OR)_4 + 4\ H_2O \rightarrow Si(OH)_4 + 4$ R-OH.

The cause for the bigger particles in MSN-3 was attributed to higher particle growth rate than the nucleation rate as a result of a faster reaction since hydrolysis of the precursor and condensation of nanoparticles is supported by the high concentration of the catalyst. These findings agree well with previous work by Kobler and Bein (2008). Previous research by Wen *et al., (*2005) attributed particle aggregation to siloxane bond formation between free hydroxyl groups. Aggregation is always energetically favored over nanoparticles since it minimizes surface areas and saturates the bonding and co-ordination sites and therefore, in order to prevent the nanoparticles from

further growth or aggregation, the particle surfaces should be saturated immediately after nucleation by electrostatic or steric stabilization (Feldmann and Goesmann, 2010).

According to Stober *et al*., (1968), the precursor concentration influences both the growth of seeds and the nucleation rate and thus the number of initial seeds. The amount of precursor added in a synthesis is of paramount significance, thus, it has to be kept in a certain range which would guarantee high final product yield and desirable particle sizes. Particle formation is templated by micelles, as it is well exemplified in literature (Beck *et al*., 1992). At surfactant concentration below the critical micelle concentration, surfactants do not aggregate into micelles. Although high concentration of surfactant is usually associated with more order in a LCT synthesis, a proper balance has to be struck between it and the other reagents in order to obtain ordered mesostructures. In the study of the effects of surfactant concentration on the regularity and morphology of mesoporous silica, Coleman and Attard (2001) found out that, if the concentration of other reagents is fixed, there is an optimal concentration of surfactant below or above which order is lost. To sum it up, Palmqvist (2003) observed that, a balance of the molar concentration of all the reagents in the reaction mixture is absolutely necessary for formation of mesostructure. Previous research shows that increasing the concentration of CTAB and TEOS decreases the particle size (Nooney *et al*., 2002). In a nut shell, electron microscopy studies revealed that the particle order, size and morphology of MSNs can be tuned by varying the concentration of the reagents in a typical reaction mixture. This observation is in good agreement with the nature of mesoporous silica nanoparticles as reported in literature (Beck *et al*., 1992).

SEM and TEM microscopy studies of UMSNs revealed no significant changes in the morphology and shape of the particles after loading (Figure 1: k – 0, p – t). In loading, the mesopores of the MSN material acted as reservoirs to soak up aqueous solution of urea. The loaded urea was believed to reside in the mesopores of MSN by physically adsorbing on it and facilitated by electrostatic interactions such as hydrogen bonding between urea molecules and the silanol (Si-OH) in the mesopores. In deed, urea's high aqueous solubility reflects its ability to engage in extensive hydrogen bonding with water. Adsorption capacities of ordered siliceous materials for polar molecules at relatively low vapor pressures have been reported to be related largely to the density of surface silanol groups (Zhao *et al*., 1997).

3.1.1 FT-IR Spectra

The FT-IR spectra of MSNs and UMSNs are displayed in Figure 2. Similar vibrational bands characteristic of ordered silica are displayed at 3450 cm^{-1}, 1100 cm^{-1}, 1630 cm^{-1}, 960 cm^{-1}, 800 cm^{-1} and 450 cm^{-1} (Figure 2a). The broad band appearing at 3450 cm^{-1} was attributed to the stretching vibration of the Si-OH (silanol) groups, The 1100 cm^{-1} broad absorption bands were ascribed to Si-O-Si (siloxane) stretching vibrations while the 1630 cm^{-1}, 960 cm^{-1}, 800 cm^{-1} and 450 cm^{-1} were attributed to SiO-H bending, Si-OH bending, SiO-H symmetrical stretching and Si-O bending vibrations respectively. Similar patterns have been reported by other researchers (Zhao *et al*., 1997; Salonen *et al*., 1997). The successful loading of urea into MSN was confirmed by appearance of urea characteristic absorption bands at 1450cm^{-1} and 1680cm^{-1} (Figure 2b) ascribed to N-H asymmetric bending vibration and C=O stretching vibrations respectively. The UMSNs spectra retained most of the major absorption bands of pure MSN and free urea and no noticeable new bands were observed indicating that urea adsorption was physical.

3.1.2 Nitrogen Adsorption / Desorption Studies

Nitrogen adsorption / desorption isotherms of MSNs and UMSNs are presented in Figure 3. Three distinct adsorption / desorption sections corresponding to relative pressures of <0.3, 0.3 - 0.9 and >0.9 are notable. Small and narrow hysteresis loops are present at desorption sections corresponding to high relative pressure values. The sorption studies yielded type IV isotherms, characteristic of mesoporous materials (Sing *et al*., 1985). The hysteresis loops observed were associated with capillary condensation taking place in mesopores. Point X (Figure 3a) indicates the stage at which monolayer coverage is complete and multilayer adsorption about to begin. BJH pore size distributions are given in Figure 4 while BJH total pore volumes and BET surface areas are shown in Table 2. Narrow pore size distributions were realized in all the samples. Pore diameters increased by 0.5 – 75.5 % after loading, the expansion was considered to be the result of occupation of the pore volume by urea molecules. The pore volumes decreased by up to 99 % while the BET surface area decreases by up to 78.2 %. Significant reduction of the pore volume and surface areas confirms successful loading of the pores with urea.

3.1.3 XRD Patterns

Powder SAXRD patterns are shown in Figure 5. Three well-defined peaks at 2θ values between 1 and 8° are exhibited for MSNs. The peaks (Figure 5A) can be indexed as (100), (110), and (200) Bragg reflections, typical of hexagonal mesoporous silica. The absence of 110 and 200 peaks in MSN-3 and MSN-4 indicates that the two MSNs are less crystalline compared with the rest. The reduced intensity of the diffraction peaks after entrapment of urea as demonstrated by SAXRD patterns of UMSNs (Figure 5b) is due to pore-filling effects which lead to a reduction of X-ray scattering contrast between the pore walls and the MSNs framework (Popovici *et al*., 2010).

3.1.4 TGA/ DTA Curves

Thermal analyses results for UMSNs are shown in Figure 6. TGA curves depict some little weight loss at low temperature which can be attributed to loss of adsorbed water. In deed, this is supported by presence of endothermic peaks at <100^{O}C in the DTA curves. DTA endothermic peak at ~135°C corresponds to the melting of the pore adsorbed urea. Corresponding TGA weight loss indicates that the urea content ranged from 2.3 % - 18.5% (w/w). Any further small loss in weight at higher temperature was ascribed to loss of silanol groups from the surface of MSNs. Usually up to three Si-OH groups per nm^2 have been reported (Jie *et al*., 2011). Apart from UMSN-1 (Figure 6a), there was no significant weight loss due to disintegration of MSNs which implied that the MSNs were thermally stable.

3.2 Loading Processes

Immersion loading technique was applied to entrap urea into MSNs because of its simplicity. A driving concentration gradient was achieved by use of high concentration of urea (guest) molecules in line with previous immersion loading studies by Heikkila *et al*. (2007).

The order of urea adsorption by the MSNs was proportional to the particle and mesopore diameters (Table 2). Besides the concentration of the guest molecules, physical properties of the nanoparticles play a crucial role in loading molecules. It has already been demonstrated that particles with larger pore diameter are easier to load (Limnel *et al*., 2011). Further reports indicate that reducing the particle size increases the loading efficiency by shortening the diffusion length (Qu *et al.,* 2006, Cauda *et al*., 2008). Pore morphology is another important parameter in drug loading of mesoporous materials. Previous studies by Cauda *et al*., (2008) and Cauda *et al*., (2009) indicate that tortuous diffusion route makes the deeper parts of the particle less accessible to the drug, leading to poorer loading efficiency.

3.3 Release Profiles of Urea-loaded Mesoporous Silica Nanoparticles

The static release profiles of UMSNs in water are given in Figure 7. A two stage sustained-release patterns were observed. A burst release effect in the range of 32 % - 91 % for UMSN-3 and UMSN-4 respectively is reflected in the first 24 hours followed by slow release over the next entire period. The combined control of mesopore size and mesopore surface chemistry allows the characteristic release time to be varied. The burst release effect was attributed to urea adsorbed on the external surface of MSNs, this initial rapid release of some guest molecules in a fertilizer delivery system would be necessary in order to initiate the required immediate treatment. Continued slow release of the plant fertilizer would ensure proper nourishment is achieved and therefore help reduce cases of periodic application. The slow release pattern observed was attributed to the release of urea confined to the mesopores of MSNs. In the case of UMSN-3 with average particle diameter of ~900 nm and pore diameter of 3.3 nm, the 2nd step in the release profile was even slower possibly due to the long diffusion path of the aggregated MSNs.

The mechanism of slow release was thought to involve the percolation of water molecules into the pore channels, the water molecules would then dissolve the urea adsorbed on the channels and diffuse out. The diffusion rate would be controlled by the physical properties of MSNs and electrostatic forces between silanol groups, urea and water molecules thus allowing the steady fashion release of the trapped molecules. The drug release process is considered as a very dynamic phenomenon that involves different properties of the materials (Limnel *et al*., 2011).

4.0 Conclusions

MSNs with varied physical properties were investigated as carriers for the controlled release of fertilizer using urea as the test molecules. Loading efficiency of up to 18.5 % w/w was achieved by a simple immersion loading technique. The release profiles of the UMSNs exhibited a two-stage controlled release pattern. It was demonstrated that urea molecules could be entrapped into MSNs and be released in a slow manner, thus MSNs can be exploited as fertilizer nanocarriers for controlled delivery application. However, more studies need to be done geared towards increasing adsorption efficiencies and prolonging the release periods in order to make the nanosystems more viable for economic exploitation.

Acknowledgements

The authors are grateful to the German Academic Exchange Service (DAAD) and Jomo Kenyatta University of Agriculture and Technology (JKUAT) for supporting this work.

References

Barrett, E. P., Joyner L. G. and Halenda, P. P. (1951). The determination of pore volume and area distributions in porous substances.1. Computations from nitrogen isotherms. *J. Am. Chem. Soc.*, **73**, pp 373-380.

Beck, J. S., Vartuli, J. C., Roth, W. J., Leonowicz, M. E., Kresge, C. T., Schmitt, K. D., Chu, CT-W., Olson, D. H., Sheppard, E. W., McCullen, S. B., Higgins, J. B. and Schlenker, J. L. (1992). A new family of mesoporous molecular sieves prepared with liquid crystal templates. *J. Am. Chem. Soc.*, **114**, pp 10834-10843.

Bottini, M., Annibale, F. D., Magrini, A., Cerignoli, F., Arimura, Y., Dawson, M. I., Bergamaschi, E., Rosato, N., Bergamaschi, A. and Mustelin, T. (2007). Quantum dot-doped silica nanoparticles as probes for targeting of T-lymphocytes. *Int. J. Nanomed.*, **2**, pp 227–233.

Brunauer, S., Emmett, P. H. and Telle,r E. (1938). Adsorption of gases in multimolecular layers. *J. Am. Chem. Soc.*, **60**, pp 309-319.

Cauda, V., Argyo, C., Piercey, D. G. and Bein, T. (2011). 'Liquid-Phase Calcination' of Colloidal Mesoporous Silica Nanoparticles in High-Boiling Solvents. *J. Am. Chem. Soc.*, **133**, pp 6484–6486.

Cauda, V., Muhlstein, L., Onida, B., Bein, T. (2009). Tuning drug uptake and release rates through different morphologies and pore diameters of confined mesoporous silica. *Micropor Mesopor Mat.*, **118**, pp 435-442.

Cauda, V., Onida, B., Platschek, B., Muhlstein, L. and Bein, T. (2008). Large antibiotic molecule diffusion in confined mesoporous silica with controlled morphology. *J. Mater Chem.*, **18**, pp 5888-5899.

Chen, J., Wang, W., Xu, Y. and Zhang, X. (2011). Slow-Release Formulation of a New Biological Pesticide, Pyoluteorin, with Mesoporous Silica. *J. Agric. Food Chem.*, **59**, pp 307-311.

Coleman, N. R. B. and Attard, G. S. (2001). Ordered mesoporous silicas prepared from both micellar solutions and liquid crystal phases. Micropor Mesopor Mater., 44–45, pp 73 –80.

Cotterill, J. V. and Wilkins, R. M. (1996). Controlled Release of Phenyl urea Herbicides from a Lignin Matrix: Release kinetics and modification with urea. *Journal of agriculture and Food chemistry*, **44**, pp 2908-2912.

Feldmann, C. and Goesmann, H. (2010). Nanoparticulate Functional Materials. *Angew.chem.int.Ed.*, **49**, pp 1362-1395.

Gao C., Qiu H., Zeng W., Sakamoto Y., Terasaki O., Sakamoto K., Chen Q. and Che S. (2006). Formation mechanism of anionic surfactant–templated mesoporous silica. *Chem. Mater.*, **18**: pp 3904-3914.

Gerion, D., Herberg, J., Bok R., Gjersing, E., Ramon, E., Maxwell, R., Kurhanewicz, J., Budinger, T. F., Gray, J. W., Shuman, M. A. and Chen, F. F. (2007). Paramagnetic silica-coated nano-crystals as an advanced MRI contrast agent. *J. Phys. Chem.*, C **111**, pp 12542–12551.

Graf, C., Dembski, S., Hofmann, A. and Ruehl, E. (2006). A general method for the controlled embedding of nanoparticles in silica colloids. *Langmuir*, **22**, pp 5604–5610.

Heikkila, T., Salonen, J., Tuura, J., Kumar, N., Salmi, T., Murzin, D. Y., Hamdy, M. S., Mul, G., Laitinen, L., Kaukonen, A. M., Hirvonen, J. and Lento, V. P. (2007). Evaluation of mesoporous TCPSi, MCM-41, SBA-15, and TUD-1 materials as API carriers for oral drug delivery. *Drug Deliv.*, **14**, pp 337-347.

Hoffmann, F., Cornelius, M., Morell, J. and Froba, M. (2006). Silica-Based Mesoporous Organic–Inorganic Hybrid Materials. *Angew. Chem. Int. Ed.*, **45**, pp 3216 – 3251.

Jie, C., Wei, W., YuQuan, X. and Xuehong, Z. (2011). Slow – Release Formulation of a New Biological Pesticide, Pyoluteorin, with Mesoporous Silica. *Journal of Agricultural and Food Chemistry*, **59**, pp 307 – 311.

Kale, S. N., Mona, J., Dhobale, S., Thite, T. and Laware, S. L. (2011). Intramolecular and Intermolecular Crosslinked Poly (vinyl alcohol)–Borate Complexes for the Sustained Release of Fertilizers and Enzymes. *Journal of Applied Polymer Science*, DOI 10.1002/app.

Kobler, J. and Bein, T. (2008). Porous Thin Films of Functionalized Mesoporous Silica Nanoparticles. *ACS NANO*, **2**(11), pp 2324-2330.

Kobler, J., Moller, K. and Bein T. (2008). Colloidal Suspensions of Functionalized Mesoporous Silica Nanoparticles. *ACS NANO*, **2**(4), pp 791-799.

Limnell, T., Santos, H. A., Makila, E., Heikkila, T., Salonen, J., Murzin, D. Y., Kumar, N., Laaksonen T., Peltonen L. and Hirvonen J. (2011). Drug Delivery Formulations of ordered Mesoporous Silica: Comparison of Three Drug loading methods. *J. Pharm. Sci.* Published online, DO1.10.1002/ jps.22577.

Liu, R., Liao, P., Liu, J. and Feng, P. (2011). Responsive polymer-coated mesoporous silica as PH – sensitive nanocarrier for controlled release. *Langmuir*, **27**, pp 3095 – 3099.

Madliger, M., Gasser, C. A., Schwarzenbach, R. P., Sander, M. (2011). Adsorption of transgenic insecticidal cry1Ab protein to silica particles. Effects on transport and bioactivity. *Enviro. Sci. Technol*., xxxx(xxx): 000-000.

Miller, J. C., Serrato, R. M., Represa-Cardens, J. M., Kundahl, G. A. (2005). *The Handbook of Nanotechnology*, John Wiley and Sons, Inc., 13-22.

Naik, S. P., Elangovan, S. P., Okubo, T., Sokolov, I. (2007). Morphology control of mesoporous silica particles. *J.Phys.Chem*., C **111**, pp 11168-11173.

Nooney, R. I., Thirunavukkarasu, D., Chen Y., Joseph, R. and Ostafin, A. E. (2002). Synthesis of Nanoscale Mesoporous Silica Spheres with controlled particle size. *Chemistry Mater.*, **14**, pp 4721-4728.

Palmqvist, A. E. C. (2003). Synthesis of ordered mesoporous materials using surfactant liquid crystals or micellar solutions. *Curr. Opin. Colloid. Interface Sci.,* **8**, pp 145–155.

Popat, A., Hartono, S. B., Stahr, F., Liu, J., Qiao, S. Z., Lu, G. Q. (2011). Mesoporous silica nanoparticles for bioadsorption, enzyme immobilization, and delivery carriers. Nanoscale, DOI: 10.1039/c1nr10224a.

Popovici, R. F., Seftel, E. M., Mihai, G. D., Popovici, E. and Voicu, V. A. (2010). Controlled Drug Delivery System Based on Ordered Mesoporous Silica Matrices of Captopril as Angiotensin-Converting Enzyme Inhibitor Drug. *J. Pharm. Sci.*, **100**(2), pp 704-714.

Qu F., Zhu, G., Huang, S., Li S., Suan, J., Zhang, D., Qius, S. (2006). Controlled release of captopril by regulating the pore size and morphology of ordered mesoporous silica. *Micropor Mesopor mat.*, **92**, pp 1-9.

Salonen, J., Lehto, V. P. and Laine, E. (1997). The room temperature oxidation of porous silicon. *Appl.Surf.Sci.*, **120**, pp 191-198.

Sing K. S. W., Everett D. H., Haul R. A. W., Moscou L., Pierotti R. A., Rouquerol J. and Siemieniewska T. (1985). Reporting physisorption data for gas/solid systems with special reference to the determination of surface area and porosity. *Pure Appl. Chem.*, **57**, pp 603-619.

Stober, W., Fink A., Bohn E. (1968). Controlled Growth of Monodisperse Silica Spheres in the Micron size range. *J. Colloid Interface Sci.*, **26**, pp 62 – 69.

Wen, L-X, Li Z-Z, Zou, H-K, Liu, A-Q and Chen, J-F (2005). Controlled release of avermectin from porous hollow silica nanoparticles. *Pest Manag. Sci.*, **61**, pp 583 – 590.

Zhao, X. S., Lu, G. Q., Whittaker, A. K., Millar, G. J. and Zhu, H. Y. (1997). Comprehensive Study of Surface Chemistry of MCM-41 Using 29Si CP/MAS NMR, FTIR, Pyridine-TPD, and TGA. *J. Phys. Chem.*, **B101**: pp 6525-6531.

Zhu M. Q., Han, J. J., Li Alexander, D. Q. (2007). CdSe/CdS/SiO_2 core/shell/shell nanoparticles. *J. Nanosci. Nanotechnol*., **7**, pp 2343–2348.

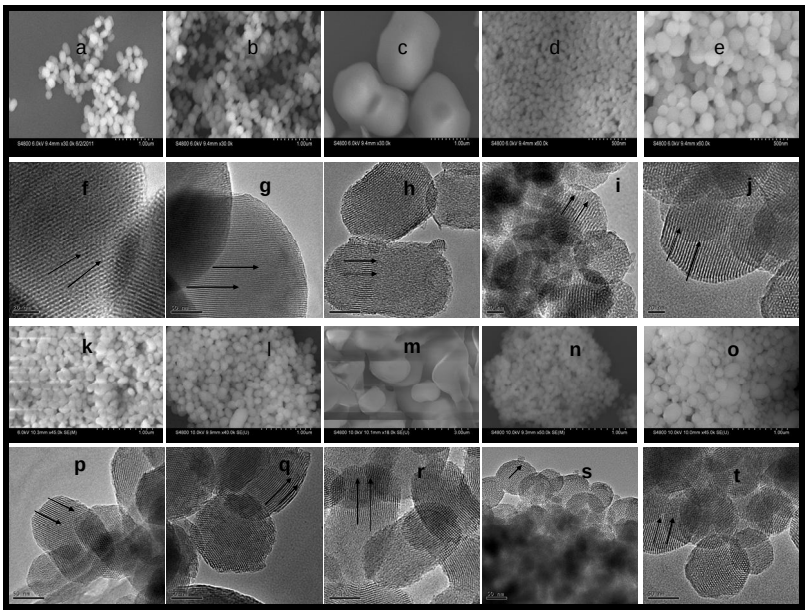

Figure 1: SEM images of MSNs (a – e), UMSNs (k – o), corresponding TEM images of MSNs (f – j) and UMSNs (p – t). Varied particle sizes and degrees of monodispersity are exhibited. Honey comb-like structure is revealed by TEM. Arrows indicate the position of channels

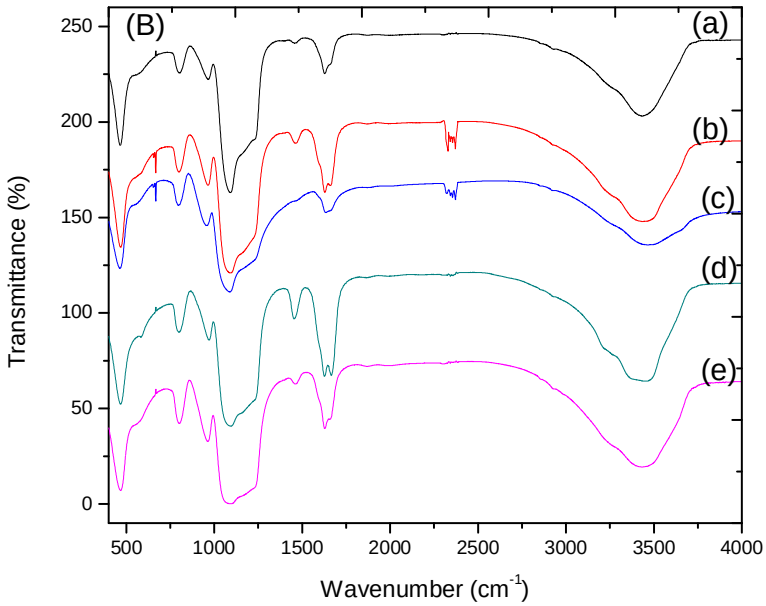

Figure 2: FT-IR spectra of MSNs (A) and UMSNs (B). Characteristic vibrational modes of typical MSN materials are exhibited in all the cases. The successful loading of urea into MSN was confirmed by appearance of urea characteristic absorption bands at 1450cm^{-1} and 1680cm^{-1}

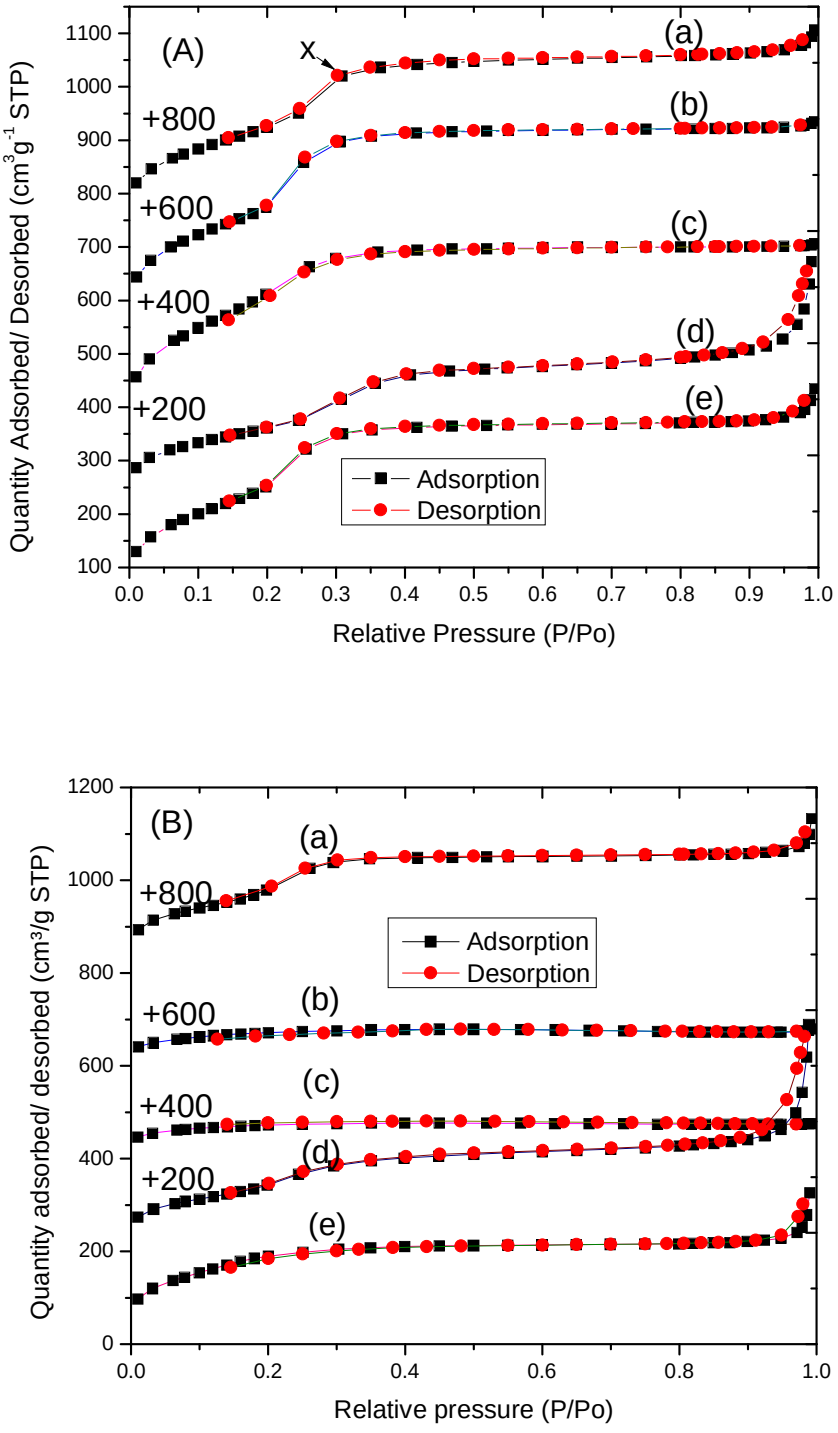

Figure 3: Nitrogen sorption isotherms of MSNs (A) and UMSNs (B). Type IV isotherms typical of mesoporous silica are exhibited

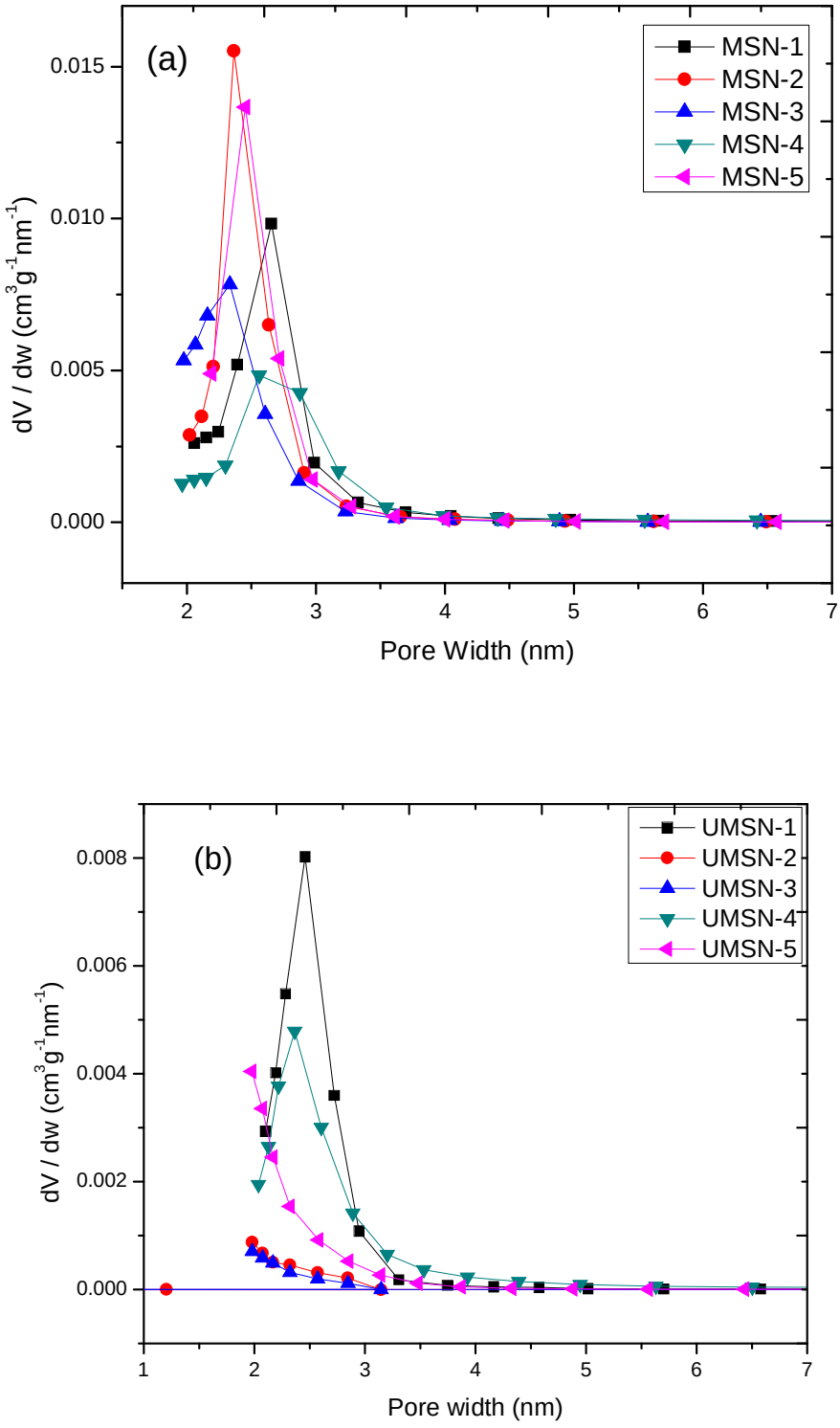

Figure 4: BJH pore size distributions of MSNs (a) and UMSNs (b). Average pore diameters expanded after urea loading

Table 2: Physical properties of MSNs and UMSNs. Particle diameters were estimated from SEM and TEM images. Pore diameters increased while surface areas and pore volumes decreased after loading MSNs with urea

Sample	Average particle diameter (nm)	Average pore diameter (nm)[a]	Surface area (m^2/g)[b]	Total pore volume (cm^3/g)[c]
MSN-1	150	2.9	825	0.74
UMSN-1	150	3.1 (5.1)*	662 (19.8)**	0.61 (16.8)**
MSN-2	200	2.5	1013	0.81
UMSN-2	200	2.5 (0.5)*	258 (74.5)**	0.09 (89.5)**
MSN-3	900 (aggregate)	2.4	1163	0.61
UMSN-3	900	3.3 (30.6)*	254 (78.2)**	0.01 (99.0)**
MSN-4	50	4.4	589	0.79
UMSN-4	50	5.3 (30.9)*	528 (10.4)**	0.82 (3.1)*?
MSN-5	100	2.9	928	0.81
UMSN-5	100	4.3 (75.5)*	713 (23.1)**	0.39 (52.1)**

* Increase (%)
** Decrease (%)
[a] BJH average pore diameter
[b] BET surface area.
[c] BJH total pore volume

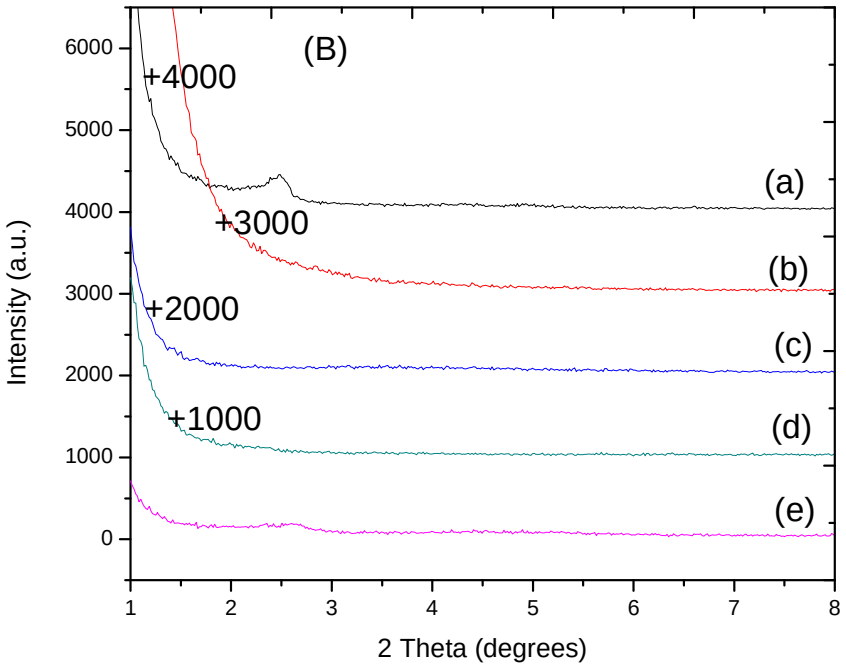

Figure 5: Powder SAXRD patterns of MSNs (A) and UMSNs (B). Presence of peaks indicates well ordered mesopores. Reduction of peak intensity in B is as a result of loading urea molecules into the MSN mesopores which reduces the X-ray scattering contrast between pore walls and pore space

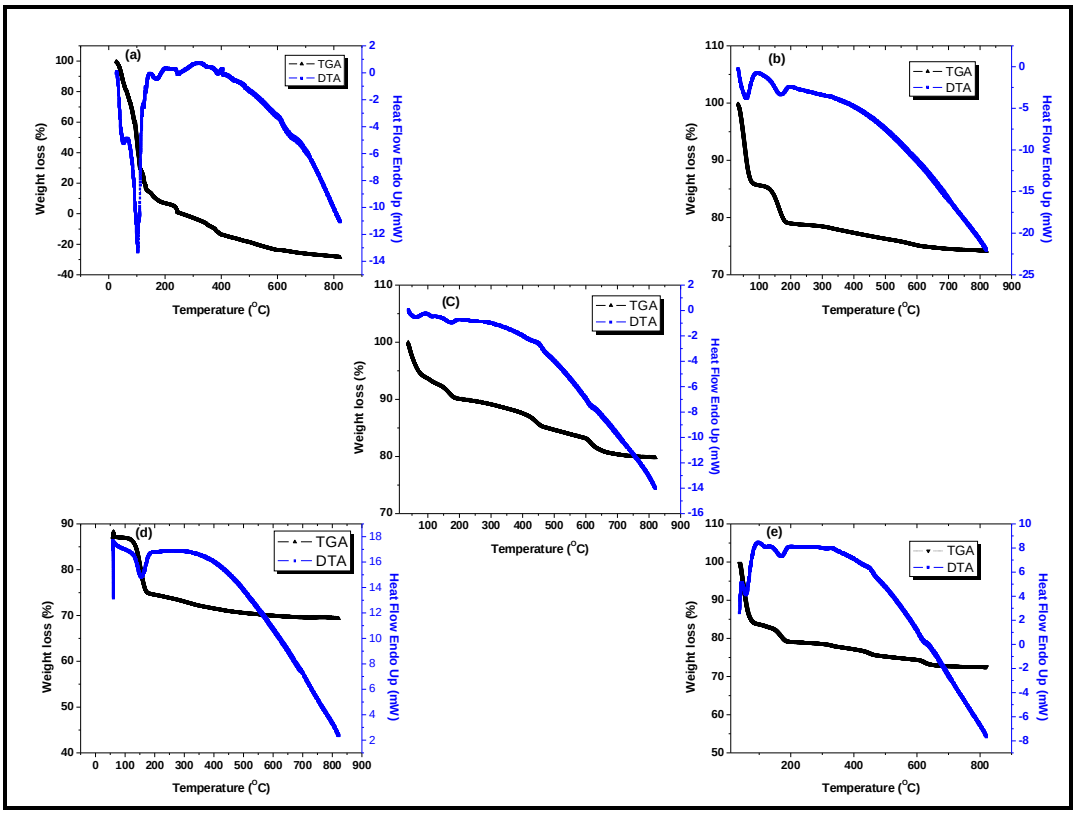

Figure 6: TGA and corresponding DTA curves for UMSNs. DTA Endothermic peaks at ~ 135°C are due to urea melting

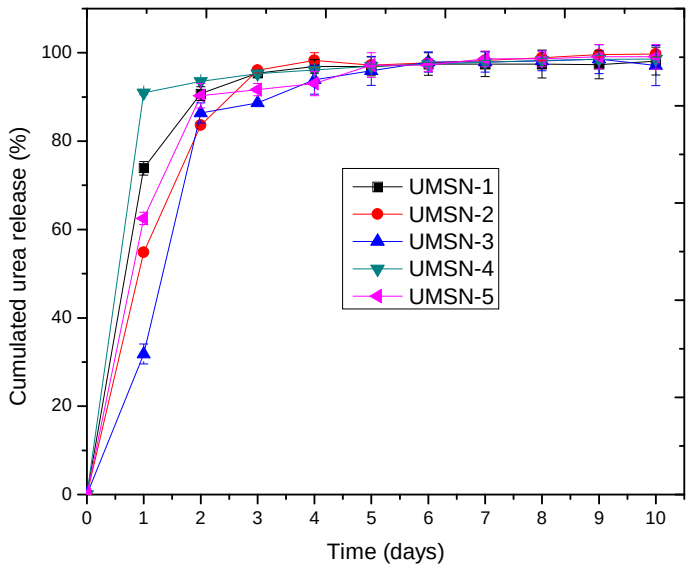

Figure 7: Static in vitro release profile of UMSNs. Slow and sustained release is shown